Quantum Well Lasers—Gain, Spectra, Dynamics

Y. ARAKAWA, MEMBER, IEEE, AND A. YARIV, FELLOW, IEEE

(Invited Paper)

Abstract—**We discuss a number of theoretical and experimental issues in quantum well lasers with emphasis on the basic behavior of the gain, the field spectrum, and the modulation dynamics. It is revealed that the use of quantum well structures results in improvement of these properties and brings several new concepts to optical semiconductor devices.**

I. Introduction

THE ability to fabricate single quantum well (SQW) and multiple quantum well (MQW) devices has given rise to new optical and electronic devices as well as to new physical phenomena [1]. Since the first investigation of optical properties in quantum wells by Dingle *et al.*, [2] the application of quantum well structures to semiconductor laser diodes [3], [4] has received considerable attention because of physical interest as well as its superior characteristics, such as low threshold current density [5], [6], low temperature dependence of threshold current [7]–[9], lasing wavelength tunability, and excellent dynamic properties [10]–[12]. By controlling the width of the quantum wells, one can modify the electron and hole wavefunctions, which leads to the modification of material parameters. This results in improvements of the laser characteristics, as well as introduction of new concepts to semiconductor optical devices.

In this paper, we describe the basic properties of the quantum well laser with emphasis on its dynamic and spectral properties as well as gain characteristics. We also discuss new device concepts including a Q-switched quantum well laser [13] and a quantum wire laser [9], [10].

II. Gain and Threshold Current

A. Density of States

In a quantum well (QW) structure, a series of energy levels and associated subbands are formed due to the quantization of electrons in the direction of the QW thickness. The density of states (per unit energy and area) of such confined electrons in a SQW structure is given by

$$\rho_c(E) = \sum_{n=1}^{\infty} \frac{m_c}{\pi\hbar^2} H[E - \epsilon_n] \tag{1}$$

where $H[x]$, m_c, $\hbar$, and ϵ_n are the Heaviside function, the effective mass of electrons, Planck's constant (h) divided by 2π, and the quantized energy level of electrons in the nth subband of the QW, respectively. When the barriers are sufficiently high and the barrier thickness is sufficiently large, ϵ_n is equal to

$$\epsilon_n = \frac{(n\pi\hbar)^2}{2m_c L_z^2} \tag{2}$$

where L_z is the thickness of the QW.

If we use a MQW structure instead of the SQW, the density of states is modified. When barrier layers between wells are thick enough, each well is independent. In this case, the density of states is just N times density of states of electrons in an SQW.

$$\rho_c(E) = N \sum_{n=1}^{\infty} \frac{m_c}{\pi\hbar^2} H[E - \epsilon_n] \tag{3}$$

where N is the number of QW's. On the other hand, if the barrier is sufficiently thin or its barrier height is small enough so that coupling between adjacent wells is substantial, the quantized energy levels are no longer degenerate, and each single well level splits into N different energy levels. In this case, the density of states (per unit energy and area) is expressed by

$$\rho_c(E) = \sum_{n=1}^{\infty} \sum_{k=1}^{N} \frac{m_c}{\pi\hbar^2} H[E - \epsilon_{nk}] \tag{4}$$

where ϵ_{nk} ($k = 1, \cdots, N$) are the energy levels which split from a single well energy level. Kroemer *et al.* [14] and Yariv *et al.* [15] analytically estimated the energy broadening due to this coupling. The coupling is important for obtaining a uniform carrier distribution in the MQW structure. However, strong coupling leads to the smearing of the configuration of the density of states and a resulting reduction in the two-dimensional character of the wells. We can characterize the smearing due to coupling by ΔE ($\equiv \max \epsilon_{nk} - \min \epsilon_{nk}$). This ΔE corresponds to the degree to which the smearing in the density of states occurs. Since the tunneling time τ_t of electrons through a barrier is on the order of $\hbar/\Delta E$, the following relations

Manuscript received January 5, 1986; revised April 11, 1986. This work was supported by the U.S. Air Force Office of Scientific Research, the U.S. Office of Naval Research, the I.T.T. Corporation, and the Japan Society for the Promotion of Science.

Y. Arakawa is with the California Institute of Technology, Pasadena, CA 91125, on leave from the Institute of Industrial Science, University of Tokyo, Minato-ku, Tokyo 106, Japan.

A. Yariv is with the California Institute of Technology, Pasadena, CA 91125.

IEEE Log Number 8609366.

are required for obtaining good uniformity of carrier concentration and maintaining the two-dimensional properties [14]:

$$\hbar/\tau_r \ll \Delta E(=\hbar/\tau_t) \ll \hbar/\tau_{\text{in}} \tag{5}$$

where τ_r is the carrier recombination time at lasing and τ_{in} is the intraband relaxation time (i.e., T_2 time). The first inequality indicates that the tunneling time for uniform carrier distribution should be much smaller than the recombination time. The second one implies that the smearing due to the coupling should be much smaller than the smearing due to the carrier relaxation effects. A localization effect in two slightly asymmetric wells is also discussed by Lang *et al.* [16] and Yariv *et al.* [15]. In order to simplify the discussion in this paper, we assume that the coupling in an MQW is weak enough that the density of states can be described by (3).

B. Linear Gain

The gain properties in QW lasers have been investigated using different theoretical treatments [17]–[23]. The main features of the gain properties in QW lasers are the gain flattening effect, dependence on the number and the thickness of the QW's and the anisotropy of the momentum matrix element. When the recombination is dominated by the band-to-band radiative process [24], [25], the linear bulk gain derived under k-selection rule is given by [26]

$$g(E, n) = \frac{\omega}{n_r^2}\chi_I(E, n) \tag{6}$$

$$\chi_I(E, n) = \int \sum_{n=0}^{\infty} \sum_{j=l,h} \rho^j_{\text{red}_n}(\epsilon)\,(f_c(E_{c_n}) - f_v(E_{v_n}))\,\hat{\chi}_I^{n,j}(E, \epsilon)\,d\epsilon. \tag{7}$$

The bulk gain is the gain exercised by an electromagnetic field if it were completely confined to the QW (i.e., a confinement factor of unity). E is the photon energy, j designates either light holes (l) or heavy holes (h), $\rho^j_{\text{red}_n}$ is the reduced density of states which is defined by $\rho^j_{\text{red}_n} = ((\rho_{c_n})^{-1} + (\rho^j_{v_n})^{-1})^{-1}$, $\rho^j_{v_n}$ is the density of states of light holes ($j = l$) or heavy holes ($j = h$), and f_c (f_v) is the quasi Fermi–Dirac distribution function for electrons (holes) in the conduction band (the valence band) with the Fermi-energy ϵ_{f_c} (ϵ_{f_v}). E_{c_n} and $E^j_{v_n}$ are equal to $(m_c\epsilon^j_{v_n} + m^j_v E + m^j_v\epsilon_{c_n})/(m_c + m^j_v)$ and $(m_c\epsilon^j_{v_n} - m_c E + m^j_v\epsilon_{c_n})/(m_c + m^j_v)$, respectively, where m^j_v and $\epsilon^j_{v_n}$ are the effective mass and the energy level of the nth subband of light holes ($j = l$) or heavy holes ($j = h$). $\chi_I(E, n)$ is the imaginary part of the susceptibility and $\hat{\chi}_I^{n,j}(E, \epsilon)$ is the susceptibility of each electron–heavy hole pair (or electron–light hole pair) in the nth subband and is given by

$$\hat{\chi}_I^{n,j}(E, \epsilon) = \frac{\pi e^2 h}{m_0^2 c n_r E_g}\,|M_{n,j}(\epsilon)|^2_{\text{ave}}\,\frac{\hbar/\tau_{\text{in}}}{(E - \epsilon)^2 + (\hbar/\tau_{\text{in}})^2} \tag{8}$$

where n_r is the refractive index of the active layer, e is the electron charge, m_0 is the mass electrons, c is the light velocity, and E_g is the bandgap. Although the possibility of the transition with no k-selection rule [19] and a violation of the $\Delta n = 0$ selection rule have been discussed, we will adopt the formula with k-selection rule with $\Delta n = 0$ selection rule.

In QW structures, it was observed by Kobayashi *et al.* [27] that the internal gain depends on the polarization of the light. Asada *et al.* [28] and Yamanishi *et al.* [29] discussed this phenomenon using the $\boldsymbol{k} \cdot \boldsymbol{p}$ perturbation method developed by Kane [30]. For instance, $|M_{n,j}|^2_{\text{ave}}$ for the TE mode (polarized parallel to the layers) due to an electron–heavy hole transition is given by

$$|M_{n,h}|^{2\text{TE}}_{\text{ave}} = |M_0|^2_{\text{ave}}\,(1 + E/(\epsilon_{c_n} - \epsilon^h_{v_n})) \tag{8}$$

where $|M_0|^2_{\text{ave}}$ is the square of the dipole matrix element of conventional double heterostructure (DH) lasers and is approximately equal to $1.33\,m_0 E_g$. For more precise discussion on this matrix element, nonparabolicity and anisotropy of valence band should be considered, which is discussed elsewhere. The calculated results shown below are, however, on the basis of the above simple model.

The quasi-Fermi energy levels ϵ_{F_c} and ϵ_{F_v} in a laser are determined by both the charge neutrality condition and the condition that the modal gain $g_{\text{mod}}(E) = \Gamma g(E)$ where Γ is the optical confinement factor) at the photon energy E_l for the laser oscillation is equal to the total losses α_{total} as follows:

$$g_{\text{mod}}(E_l) = \Gamma g(E) = \alpha_{\text{total}} = \Gamma\alpha_{\text{ac}} + (1 - \Gamma)\,\alpha_{\text{ex}} + L^{-1}\ln(1/R) \tag{9}$$

where α_{ac}, α_{ex}, R, and L are the loss in the active region, the loss in the cladding layers, the reflectivity, and the cavity length, respectively.

Once the Fermi energy levels are fixed, the injected current density J is determined by the following equation:

$$J = eN\left(\int\int \frac{8\pi n_r^2 E_g^2}{c^2 h} \sum_{n=0}^{\infty} \sum_{j=l,h} \rho_{\text{red}_j}(\epsilon)\, f_c(E_{c_n}) \cdot (1 - f_v(E_{c_n}))\,\hat{\chi}_I^{n,j}(E, \epsilon)\,d\epsilon\,dE\right). \tag{10}$$

The optical confinement factor Γ depends strongly on the structure. If we use the separate confinement structure, Γ can be expressed approximately by the following simple formulas [11]:

$$\Gamma = 0.3N\frac{L_z}{L_0} \tag{11}$$

where N is the number of QW's, L_0 is equal to 1000 Å, and the following structure is assumed; the MQW laser has $Ga_{0.75}Al_{0.25}As$ barriers and $Ga_{0.75}Al_{0.25}As$ waveguide layers, and the dimension of the waveguide layers is determined so that the total thickness, including QW's, barriers, and waveguide layers, is equal to 2000 Å. The cladding layers are made of p-$Ga_{0.6}Al_{0.4}As$ and n-$Ga_{0.6}Al_{0.4}As$. In the following calculation, we will ignore

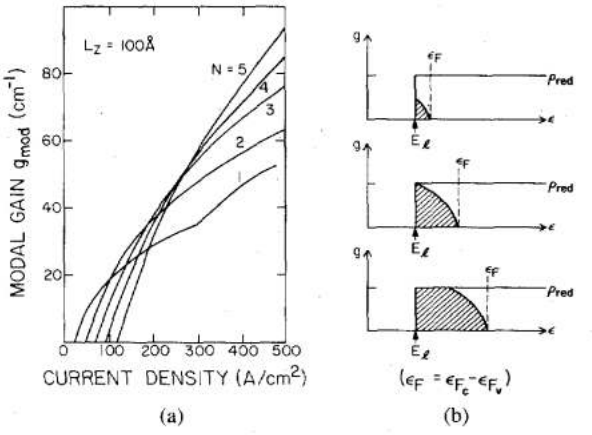

Fig. 1. (a) The modal gain g_{mod} ($=\Gamma g$) as a function of the injected current density with various number of quantum wells N. The thickness of each quantum well is assumed to be 100 Å. (b) An illustration which explains how the gain flattening effect occurs with the increase of the Fermi energy levels.

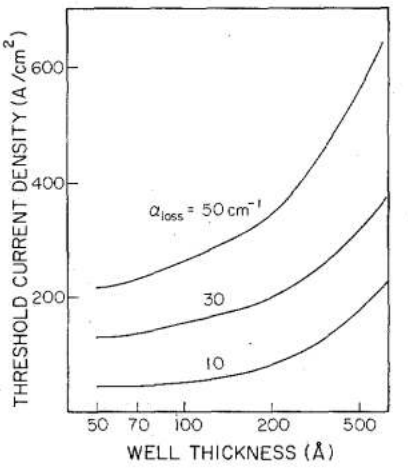

Fig. 2. The threshold current as a function of the quantum well thickness with various total loss α loss. The number of quantum wells is optimized so that the threshold current is minimum.

nonradiative effects such as the Auger recombination and the intervalence band effect [31]–[34].

If the carrier density, hence the quasi-Fermi energy level, in each QW is the same, the modal gain with N QW's, $g_{mod}^N(E_l)$, is given by

$$g_{mod}^N(E_l) = N g_{mod}^{(N=1)}(E_l) \tag{12}$$

where E_l is the lasing photon energy. But, this, of course, happens at

$$J^N = N J^{(N=1)} \tag{13}$$

or, stated in words, the modal gain available from N QW's is N times that of an SQW and is obtained at a current density which is N times that of an SQW laser. Fig. 1(a) shows the calculated modal gain $g_{mod}^N(E_l)$ as a function of the injected current density in a QW laser with N QW's on the basis of (12) and (13). We notice a very marked flattening (''saturation'') of the gain at high injected currents, especially in an SQW ($N = 1$). This gain flattening effect is due to the step-like shape of the density of states functions, and the fact that once the quasi-Fermi energy levels penetrate into the conduction band and valence band, which happens at high injected currents, the product $\rho_{red}(\epsilon)(f_c - f_v)$, which determines the gain, becomes a constant and no longer increases with the current. This is illustrated in Fig. 1(b). This flattening effect was evidenced recently by Arakawa *et al.* [35] in a systematic measurement of the threshold current of high-quality GRIN-SCH (graded index waveguide-separate confinement heterostructure) SQW lasers of different cavity length. They observed the jump of the lasing wavelength with the decrease of the cavity length from the wavelength corresponding to $n = 1$ transition to the wavelength corresponding to $n = 2$ transition, which demonstrates the existence of discrete quantized energy levels.

Owing to this gain flattening effect, there exits an optimum number of QW's for minimizing the threshold current for a given total loss α_{total}. From Fig. 1(a), we see that, for low losses, the injected threshold current is minimum with $N = 1$. On the other hand, if $\alpha_{total} = 20\ cm^{-1}$, the threshold current with $N = 1$ is larger than that of $N = 2$. At higher values of α_{total} which call for larger laser modal gain, a larger number of wells is needed. When α_{total} is 50 cm^{-1}, a five-well structure ($N = 5$) will have the lowest threshold current.

Fig. 2 shows the threshold current as a function of the QW thickness for various α_{total}. In this calculation, the number of QW's is optimized for each QE thickness so that the threshold current is minimum. The results indicate that the threshold current of thinner QW lasers (L_z = 50–100 Å) is much lower than that of thicker QW lasers. We also notice that the threshold current is minimized with $L_z \approx 60$ Å when α_{loss} is low (α_{loss} = 10–30 cm^{-1}). This is mainly due to the fact that the current for transparency (gain equals to zero) is minimized at the thickness of $L_z \approx 60$ Å in the case of $N = 1$ and also due to the fact that the optimum N in QW lasers with each thickness is 1 in the case of low α_{total} for thin QW structures.

C. Experiment

Many experiments on GaAs/GaAlAs QW laser [5], [7], [36]–[43], InGaAsP/InP QW lasers [44]–[47], InGaAlAs QW lasers [48], and AlGaSb QW lasers [49] have been reported. Fuji *et al.* [5] reported a very low threshold current density as low as 175 A/cm^2 with 480 μm cavity length in a GaAs/AlGaAs GRIN-SCH SQW laser. This demonstrates the realization of high gain with lower spontaneous emission rate owing to the step-like density of states.

sulting in a red shift of the excitonic absorption energy. The band discontinuities prevent the ionization of the exciton, allowing excitonic resonances to be observed at room temperature with large applied fields ($> 10^5$ V/cm).

The concept of the size effect modulation proposed by Yamanishi *et al.* [74] also utilizes the application of electric field. This causes the spatial of the electron distribution and hole distribution in a well, which leads to the modulation of the matrix elements.

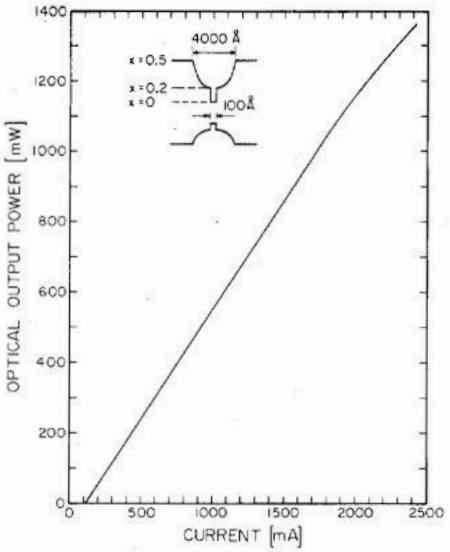

Fig. 3. The light output power versus injection current under pulsed condition of a 100 μm wide and 480 μm broad area GaAs/AlGaAs GRIN-SCH laser (400 ns, 25 Hz).

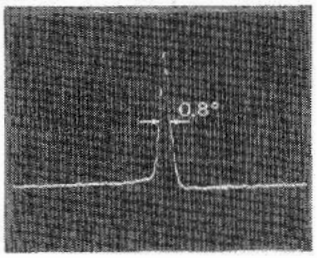

Fig. 4. The far-field pattern parallel to the injection plane of a 100 μm wide broad area GaAs/AlGaAs GRIN-SCH laser at $I = 1.2I_{th}$. The measured full width at half maximum is 0.8° which is quite close to the diffraction limit of 0.4°.

Recently, in MBE-grown broad area GaAs/AlGaAs GRIN-SCH SQW lasers, a quantum efficiency around 70 percent with a single far-field lobe as narrow as 0.8° has been achieved by Larsson *et al.* [50]. Fig. 3 shows the measured light output power versus injection current under pulsed condition (400 ns, 25 Hz) using calibrated Si photodiodes and filters. The threshold current is 110 mA, which corresponds to a threshold current density of 230 A/cm^2. The maximum output power of 1.35 W from one mirror was limited by the available current from current source. The high external quantum efficiency is a combined result of the low threshold current density and the high differential quantum efficiency of 84 percent. This can be explained in terms of the step-like density of states associated with the quasi-two-dimensional structure of the SQW, enhanced carrier and optical confinement in the GRIN region, and optimized growth conditions. The internal loss estimated by measuring the differential quantum efficiency of the lasers with various cavity length is as low as 1.8 cm^{-1}. Fig. 4 shows the far-field pattern parallel to the junction plane for a 100 μm wide laser at $I = 1.2I_{th}$ where I_{th} is the threshold current. The measured full width at half maximum (FWHM) is 0.8°, to be compared to the diffraction limit of 0.4°. This extremely narrow far field is a result of increased lateral coherence produced by uniformly distributed and phase-locked filaments.

III. Differential Gain and Modulation Bandwidth

A. Relaxation Oscillation Frequency and Differential Gain

The direct modulation of a semiconductor laser has been a subject of active research for the past 20 years [51]–[55]. Experiments have shown the existence of a resonance peak in the modulation response. In the early stage of the semiconductor laser development, the principal concern was in optimizing structures for realizing low threshold currents and high quantum efficiencies. With the increasing sophistication of the laser and the maturing of the technology, their high-speed dynamic characteristics became a subject of increasing importance. Many efforts have been devoted to realizing a wide bandwidth in conventional DH semiconductor lasers by changing the laser geometry. Another approach is to modify the basic material properties through the use of QW structures. In this section, we discuss the possibility of the improvement of these characteristics.

The relaxation oscillation corner frequency f_r gives the useful direct modulation bandwidth of a semiconductor laser. The simple rate equation for laser dynamics can be described as follows:

$$\frac{dn}{dt} = \frac{J(t)}{eL_z} - \frac{n_r}{c} g(n, E_l)\, P - \frac{n}{\tau_s} \tag{14}$$

$$\frac{dP}{dt} = \Gamma \frac{n_r}{c} g(n, E_l)\, P + \beta \frac{n}{\tau_s} - \frac{P}{\tau_p} \tag{15}$$

where P is the photon density, β is the spontaneous emission coefficient into the lasing mode, τ_s is the carrier lifetime, $J(t)$ (cm^{-2}) is the injected current density, n is the carrier concentration, and $g(n, E_l)$ (cm^{-2}) is the bulk gain, while $\Gamma g(n, E_l)$ is the modal gain as a function of the carrier density n at the lasing photon energy E_l. To emphasize the dependence of the gain on carrier concentration, we denote the gain as $g(E, n)$ hereafter. When we discuss the carrier density in QW structures, we usually use the two-dimensional density (per cm^2). However, the proper "bookkeeping" of photons and carriers requires that n stand for carrier density per unit volume. The relaxation resonance frequency f_r is determined by a small-signal analysis of (14) and (15). The result can simply be expressed by [53]

$$f_r = \frac{1}{2\pi} \sqrt{\frac{n_r g'(E_l, n)}{c} \frac{P_0}{\tau_p}} \tag{16}$$

where P_0 is the stationary photon density in the cavity and $g'(E_l, n)$ is the differential gain (i.e., $g'(E, n) = \partial g(E, n)/\partial n$). This result suggests several ways to improve f_r: larger $g'(E_l, n)$, smaller τ_p, and larger P_0. The reduction of τ_p and the increase of P_0 are realized with the use of short cavity lasers [53] and window-type lasers [54]. To

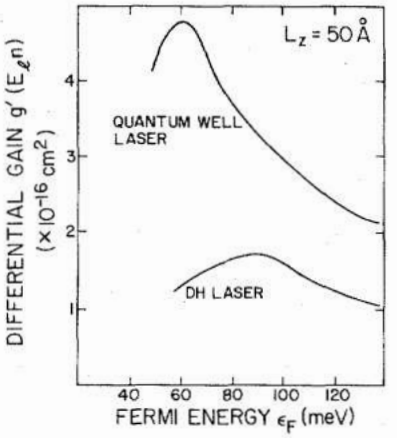

Fig. 5. The differential gain as a function of the conduction band quasi-Fermi energy level in a conventional double heterostructure laser and a quantum well laser with 50 Å well thickness.

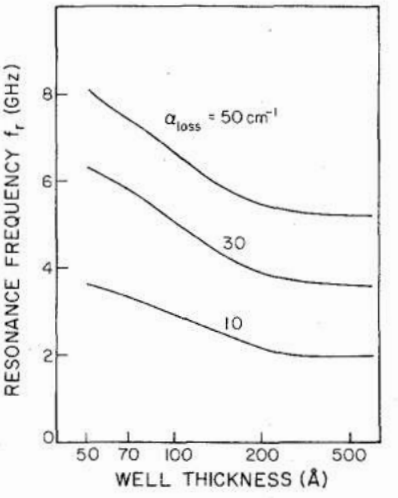

Fig. 6. The relaxation resonance frequency in a quantum well laser as a function of the well thickness. The number of quantum wells and quantum wires is optimized for each quantum well thickness.

increase $g'(E_l, n)$, operation at low temperatures [55] and the use of coupled cavity lasers [56] have been considered.

The basic quantum mechanical expression for $g'(E, n)$ suggests yet another way to increase $g'(E, n)$: changing the electron density of states with the use of QW's [10], [11]. Since the gain $g(E, n)$ is proportional to the imaginary part $\chi_I(E, n)$, as shown in (6), $g'(E, n)$ can be expressed by the following equation:

$$g'(E, n) = \frac{\partial}{\partial n}\left(\frac{\omega}{n_r^2}\chi_I(E, n)\right). \tag{17}$$

It is easily seen from this equation that the density of states plays an important role in determining the properties of $g'(E, n)$ as well as $g(E, n)$. The step-like density of states narrows the gain spectrum compared to that in the bulk material, which leads to an increase of $g'(E, n)$.

Fig. 5 shows the calculated differential gain $g'(E_l, n(\epsilon_{F_c}))$ for a conventional DH laser and a QW laser as a function of the conduction band quasi-Fermi energy level ϵ_{F_c} (measured from the lowest subband energy level). The thickness of the QW structures is equal to 50 Å. The quasi-Fermi energy level for the holes is determined by the charge neutrality condition. The result predicts an enhancement of $g'(E, n)$ for the QW active layer. Note that since $g'(E_l, n)$ is a bulk parameter, it is independent of the number of QW's.

This figure also shows that $g'(E_l, n)$ depends strongly on ϵ_{F_c} (i.e., necessary excitation for laser oscillation). The Fermi energy dependence of $g'(E_l, n)$ implies that there is an optimum number N of QW's in a laser structure which causes the largest enhancement of f_r. To see this, consider, again, the threshold condition for lasing in (9). For simplicity, we ignore the dependence of α_{total} on the structure. Since the gain is a monotonically increasing function of ϵ_{F_c}, the required ϵ_{F_c} for laser oscillation decreases monotonically with the increase of N. Consequently, there exits an optimum N for realizing $\epsilon_{F_c}^{\max}$, defined to yield the maximum $g'(E_l, n)$. It is easily shown that the ϵ_{F_c} at lasing threshold for $N = 1$ is much larger than $\epsilon_{F_c}^{\max}$. Therefore, the largest $g'(E_l, n)$ and the fastest modulation speeds are achieved for the MQW cases ($N \geq 2$). Fig. 6 shows the calculated f_r as a function of L_z (the QW width); α_{total} is assumed to be 50 cm^{-1}. At each L_z, the number of wells is optimized and f_r is normalized by f_r of a conventional DH laser (i.e., $L_z \to \infty$). The results suggest that by optimizing N, f_r can be enhanced by a factor of two in thin QW lasers.

B. Experiment

The enhancement of f_r was experimentally demonstrated by Uomi *et al.* [57]. They used an MQW laser with a self-aligned structure grown by MOCVD and measured the relaxation oscillation observed in the transient characteristics without dc bias at room temperature. f_r was measured as a function of (P/P_c) where P is the output power and P_c is the power for catastrophic optical damage. It was found that f_r of the MQW laser is about twice as large as that of a DH laser with the same structure. They estimated the modulation frequency to be 11 GHz near the catastrophic optical damage limit. This experimental result supports the above theoretical calculations. Iwamura *et al.* [58] measured the longitudinal mode behavior in MQW lasers under modulation, and they obtained a result which suggest that the narrower gain spectrum of an MQW laser causes fewer longitudinal modes under modulation.

IV. Spectral Noise Properties

A. Spectral Linewidth

Recently, the subject of semiconductor laser noise has received considerable attention. The deviation of conventional DH laser noise characteristics from well-established norms was demonstrated by Fleming *et al.* [59]. They found that the linewidth varies inversely with output power, as predicted by the modified Schawlow–Townes formula. The coefficient of the power dependence, however, was significantly larger than predicted by the formula. This discrepancy was explained physically by

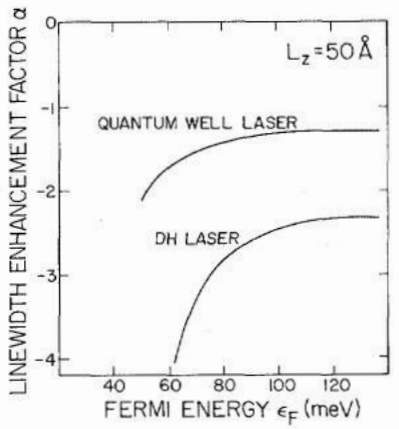

Fig. 7. The linewidth enhancement factor α as a function of the conduction band quasi-Fermi energy level in a conventional double heterostructure laser and a quantum well laser with 50 Å well thickness.

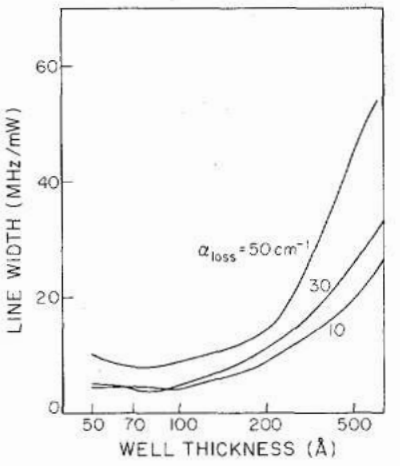

Fig. 8. The spectral linewidth in a quantum well laser as a function of the well thickness. The number of quantum wells is optimized for each quantum well thickness.

Henry [60], and a new theory was developed by Vahala *et al.* [61], [62]. They showed that the expected broadening enhancement is a factor $(1 + \alpha^2)$ where α is named the linewidth enhancement factor. The basic explanation is that phase fluctuations can result from index variations during relaxation oscillations after a spontaneous event, as well as by direct spontaneous emission events. For reducing the linewidth, the use of an external mirror, coupled cavity laser, and distributed feedback laser have been investigated. Another approach for reducing the linewidth is to modify the density of states. In this section, we indicate how the linewidth (or α) is reduced through the use of QW structures [10]–[12], [63].

The spectral linewidth $\Delta\nu$ can be expressed by [60], [61], [64]

$$\Delta\nu = \frac{v_g h\nu \Gamma_g R_m n_{sp}}{\pi P}(1 + \alpha^2) \tag{18}$$

$$\alpha = \frac{\partial\chi_R(E_l, n)/\partial n}{\partial\chi_I(E_l, n)/\partial n}. \tag{19}$$

R_m, v_g, $h\nu$, Γ, g, n_{sp}, and P are the mirror loss, the group velocity of light, the photon energy, the optical confinement factor, the bulk gain at threshold, the spontaneous emission factor, and the laser output power, respectively. $\chi_R(E, n)$ is the real part of the complex susceptibility and

$$\chi_R(E, n) = \int \sum_{n=0}^{\infty} \sum_{j=l,h} \rho^j_{red_n}(\epsilon)(f_c(E_{c_n}) - f_v(E_{v_n}))\, \hat{\chi}^{n,j}_R(E, \epsilon)\, d\epsilon$$

$$\hat{\chi}^{n,j}_R(E, \epsilon) = \frac{\pi e^2 h}{m_0^2 c n_r E_g} |M_{n,j}(\epsilon)|^2_{ave} \frac{E - \epsilon}{(E - \epsilon)^2 + (\hbar/\tau_{in})^2}. \tag{21}$$

α reflects the strong amplitude-phase coupling of the lasing field in a semiconductor laser resulting from the highly detuned optical gain spectrum. Equation (18) indicates that $\Delta\nu$ depends on the electronic density of states through α and n_{sp}.

The denominator of (19) is proportional to $g'(E_l, n)$. Therefore, from the results of the previous section, an increase of the denominator can be expected with the use of QW's. The numerator in (19), however, is also enhanced in QW structures. Therefore, it is difficult to predict the behavior of α in these structures without numerical calculations. Fig. 7 gives a calculation of α as a function of ϵ_{F_c} for conventional DH lasers and QW lasers. In this figure, the thickness of the QW's is equal to 50 Å. These calculation indicate first that α depends strongly on ϵ_{F_c} (or equivalently, on the level of injection which is determined by optical gain required for laser oscillation), its magnitude decreasing for larger ϵ_{F_c}. (This result has been observed experimentally for conventional DH lasers [65].) Second, this reduction of $|\alpha|$ with increasing excitation is larger in QW lasers than in conventional DH lasers. Therefore, a smaller number of QW's leads to a smaller value of $|\alpha|$ because a laser with a smaller number of QW's requires higher Fermi energy levels for a given modal gain.

The linewidth $\Delta\nu$ also contains the spontaneous emission factor n_{sp} which decreases monotonically with the increase of ϵ_{F_c} and converges to 1. This n_{sp} is the ratio of the spontaneous emission rate into the lasing mode to the stimulated emission rate and is given by

$$n_{sp} = \frac{\int \sum_{n=0}^{\infty} \sum_{j=l,h} \rho^j_{red_n}(\epsilon)\, f_c(E_{c_n})(1 - f_v(E_{v_n}))\, \hat{\chi}^{n,j}_I(E, \epsilon)\, d\epsilon}{\int \sum_{n=0}^{\infty} \sum_{j=l,h} \rho^j_{red_n}(\epsilon)\, (f_c(E_{c_n}) - f_v(E_{v_n}))\, \hat{\chi}^{n,j}_I(E, \epsilon)\, d\epsilon}. \tag{22}$$

If the energy broadening due to the intraband relaxation is extremely small, we can approximate n_{sp} at the photon energy E_l by

$$n_{sp} \approx \frac{1}{1 - \exp((E_l - \epsilon_{F_c} + \epsilon_{F_c})/kT)}. \tag{23}$$

As shown in this equation, n_{sp} is a monotonically decreas-

ing function of ϵ_{F_c}. Therefore, for a fixed loss (i.e., Γ_g is constant), it is advantageous to operate with a high ϵ_{F_c} to attain a reduction in $\Delta\nu$. With regard to the number of QW's, this means that, in contrast to f_r, the SQW active layer is the optimum choice for phase noise reduction. Fig. 8 gives the minimum attainable $\Delta\nu$ as a function of L_z with various α_{loss}. We notice that $\Delta\nu$ is reduced greatly for a thin active layer. $\Delta\nu$ is minimum around $L_z = 80$ Å because there is the current region in which α of $L_z = 80$ Å is smaller than that of $L_z = 50$ Å in the case of $\alpha_{\text{loss}} = 10\ \text{cm}^{-1}$. Since the value $\Delta\nu$ for a DH laser (0.1 μm active layer) is calculated to be 60 MHz/mW with $\alpha_{\text{total}} = 30\ \text{cm}^{-1}$, $\Delta\nu$ can be substantially reduced with a thin QW structure by a factor of $\frac{1}{10}$ compared to $\Delta\nu$ for DH lasers. For all L_z, $\Delta\nu$ increases monotonically when the number of QW's increases.

B. Experiments

Recently, Ogasawara *et al.* [66] measured the α parameter of MQW lasers experimentally. The active layer consisted of four 40 Å thick GaAs wells and four 50 Å thick $Al_{0.3}Ga_{0.7}As$ barriers. They measured the change in $\partial\chi_R(E_l, n)/\partial n$ and $\partial\chi_I(E_l, n)/\partial n$ separately. $\partial\chi_R(E_l, n)/\partial n$ is measured from the wavelength shift of a Fabry–Perot mode with pulsed current injection below threshold and $\partial\chi_I(E_l, n)/\partial n$ is measured from the depth of modulation in the spontaneous emission intensity. Although their measurement is not a direct measurement and the measured α is obtained below threshold, their result supports our prediction. Their experiment suggests that α of a QW laser is smaller by a factor of $\frac{1}{2}$ compared to that of a conventional DH laser with the same carrier concentration.

V. New Optical Devices Using Quantum Wells

A. New Optical Devices Using QW Structures

As discussed above, the QW laser is a promising light source for various applications, and considerable effort has been devoted to developing high-quality QW lasers. In addition, other new optical devices based on QW structures have been proposed and demonstrated. These include optical modulators [67], [68], optical bistable devices [69], tunable p-i-n QW photodetectors [70], [71], size effect modulation light sources [74], Q-switching laser light sources [9], and modulation-doped detectors [72], [73]. The first three devices utilize the quantum-confined Stark effects [84], [85] described as follows. The room-temperature absorption spectrum of MQW displays enhanced absorption at the band edge, with a double-peaked structure caused by excitons whose binding energy is enhanced by the two-dimensional confinement. When an electric field is applied to the QW's perpendicular to the layers, the exciton absorption peak shifts to lower energy. This effect is much larger than the Franz–Keldysh effect seen in bulk materials. The dominant mechanism is the decrease in confinement energies, resulting in a red shift of the excitonic absorption energy.

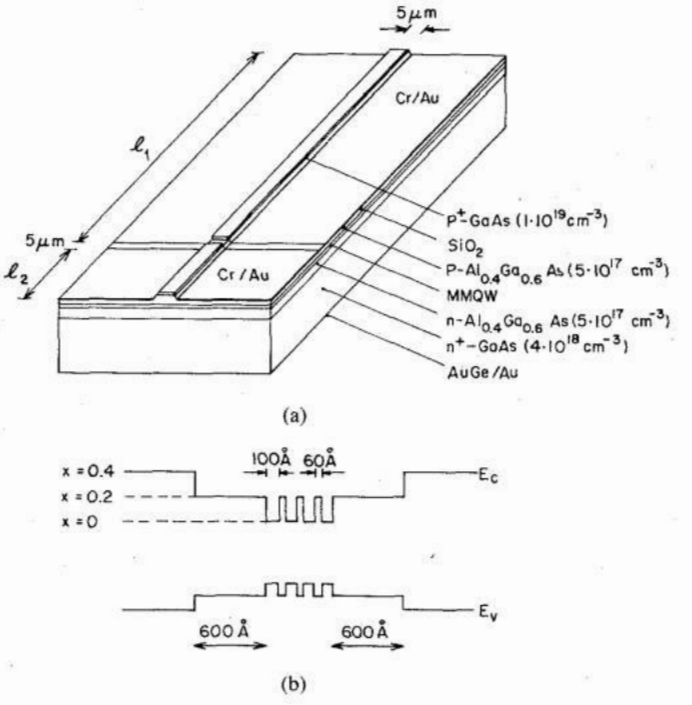

Fig. 9. (a) Perspective view of the two-segment quantum well laser. The lengths of the amplifier section l_1 and the modulator section l_2 were 250 and 50 μm, respectively. (b) The associated energy band diagram of the active layer.

The band discontinuities prevent the ionization of the exciton, allowing excitonic resonances to be observed at room temperature with large applied fields ($> 10^5$ V/cm).

The concept of the size effect modulation proposed by Yamanishi *et al.* [74] also utilizes the application of electric field. This causes the spatial displacement of the electron distribution and hole distribution in a well, which leads to the modulation of the matrix elements.

B. Q Switching in an MQW Laser with an Internal Loss Modulation

Picosecond pulse generation technology in semiconductor laser diodes is important for high-speed optical communication systems [75]–[83]. In Q-switching lasers, in contrast to mode-locked lasers, no external mirror is needed [80], [81] and lower modulation power is required compared to gain switching systems [82], [83]. Recently, effective active Q switching was successfully demonstrated by Arakawa *et al.* [13] in a GaAs/AlGaAs MQW laser with an intracavity monolithic electroabsorption loss modulator. The physical phenomena utilized are the quantum confined Stark effect in the modulation section and the enhanced carrier-induced band shrinkage effect [86] in the optical amplifier section. Optical pulses as narrow as 18.6 ps full width at half maximum (FWHM), assuming a Gaussian waveform, are generated.

Fig. 9(a) illustrates the two-segment MQW laser consisting of an optical amplifier section and an electroabsorption loss modulator section. The device structure was grown by molecular beam epitaxy. The associated energy band diagram is shown in Fig. 9(b). A 5 μm wide sepa-

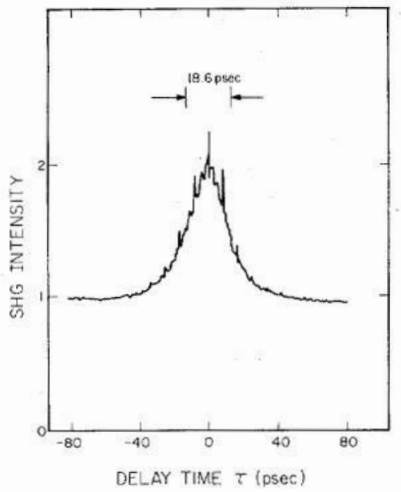

Fig. 10. Intensity autocorelation trace obtained from second harmonic generation widht 1.5 GHz modulation frequency and 0 V bias. The current injected into the optical amplifier section is 170 mA.

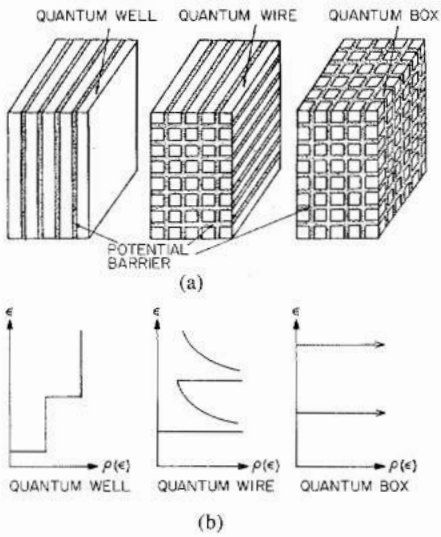

Fig. 11. (a) Illustration of the active layer with a multiquantum well structure, a multiquantum wire structure, and a multiquantum box structure, (b) Density of states of electrons in a DH structure, a multiquantum well structure, a multiquantum wire structure, and a multiquantum box structure.

ration was selectively etched in the p^+-GaAs between the two segments for electrical isolation. The lengths of the amplifier section l_1 and the modulator section l_2 were 250 and 50 μm, respectively.

In the amplifier section, the carrier-induced band shift occurs. This effect is enhanced in MQW lasers compared to conventional DH lasers, resulting in a decrease of the lasing photon energy by about 17 meV [86] compared to the absorption edge. Therefore, with no electronic field, the absorption loss is small at the lasing photon energy, which results in extremely large loss changes induced by the application of an electrical field with the quantum-confined Stark effects to the modulation section.

Q switching was obtained by applying both a dc bias voltage V_b and a microwave signal to the modulator. Fig. 10 shows an intensity autocorrelation trace obtained from the second harmonic generation under the condition of 1.5 GHz modulation frequency and $V_b = 0$. The autocorrelation FWHM is 26.3 ps, which corresponds to a pulse full width at half maximum $\Delta\tau_{1/2}$ of 18.6 ps if a Gaussian waveform is assumed.

The efficient Q switching in the two-segment MQW laser results from the following mechanisms. In the Q-switching regime, a large loss change and a high differential gain (the derivative of the gain with respect to carrier concentration) will lead to a narrow pulse width. In this device, a large loss change is realized with the quantum-confined Stark effect in the modulator section and the band shrinkage effect in the optical amplifier section. On the other hand, a high differential gain is also expected in the quasi-two-dimensional electronic system in an MQW structure [10], [11]. Thus, by the use of an MQW structure, the two-segment laser satisfies both requirements for the generation of narrow optical pulses.

The modulation frequency response (i.e., repetition rate) of the laser was also measured. We observed the fundamental spectrum as well as harmonic spectrum lines in the spectrum analyzer display. At the present stage, the maximum repetition rate which still leads to regular pulse generation is 5.2 GHz.

VI. Quantum Wire and Quantum Box Lasers and Their Experimental Demonstration

A. Concepts of Quantum Wire Laser and Quantum Box Laser

The QW structure has proved to be very promising for application to semiconductor lasers, which is due mainly to the two-dimensional properties of the carriers [9]. Arakawa *et al.* [9] proposed the concept of quantum wire lasers or quantum box lasers with, respectively, a one-dimensional or/and a zero-dimensional electronic system. They predicted a reduction in the temperature dependence of the threshold current due to the peaked structure of the density of states. In addition, the gain characteristics [87] and the dynamic properties were also investigated [10]. Although Petroff tried to fabricate quantum wire structures [88], no satisfactory quantum wire structure has been fabricated for optical devices or electronic devices [89] to date. Another approach for realizing the one- or two-dimensional effects experimentally is the use of magnetic fields [9], [90]–[95]. One-dimensional electronic systems can be formed by placing a conventional DH laser in a high magnetic field. If we place a quantum well laser in a high magnetic field so that the quantum well plane is perpendicular to the field, a zero-dimensional electronic system is realized. In this section, we discuss the possible properties obtained in quantum wire lasers and quantum box lasers theoretically and then demonstrate these effects in high magnetic field experiments.

Fig. 11(a) shows simple illustrations of the active layer in multiquantum well, multiquantum wire, and multiquantum box lasers. By making such multidimensional microstructures, the freedom of the carrier motion is re-

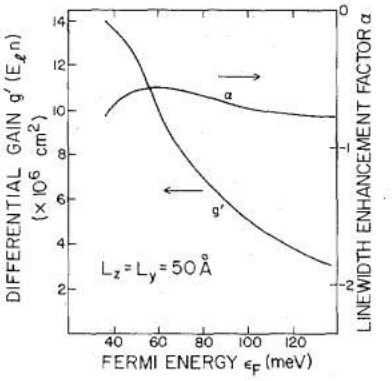

Fig. 12. The differential gain and α as a function of the conduction band quasi-Fermi energy level in a quantum wire laser with 50 Å quantum dimensions.

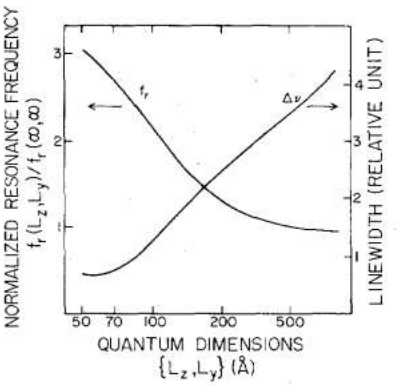

Fig. 13. The relaxation resonance frequency and the linewidth in a quantum wire laser as a function of the wire thickness. The number of quantum wells and quantum wires is optimized at each quantum well thickness.

duced to one or zero. The density of states of electrons in these structures is expressed as

$$\rho_c^{\text{wire}}(\epsilon) = \left(\frac{m_c}{2\hbar^2\pi^2}\right)^{1/2} \sum_{l,m} \frac{1}{\sqrt{\epsilon - \epsilon_l - \epsilon_m}}$$

for the quantum wire laser (24)

$$\rho_c^{\text{box}}(\epsilon) = \sum_{l,m,k} \delta(\epsilon - \epsilon_l - \epsilon_m \epsilon_k)$$

for the quantum box laser (25)

where ϵ_l, ϵ_m, and ϵ_k are the quantized energy levels of a quantum wire laser and a quantum box laser. As shown in Fig. 11(b), the density of states has a more peaked structure with the decrease of the dimensionality. This leads to a change in the gain profile, a reduction of threshold current density, and a reduction of the temperature dependence of the threshold current. Furthermore, improvements of the dynamic properties are also expected.

The narrower gain profile due to the peaked density of states leads to a high differential gain. One curve in Fig. 12 shows the differential gain as a function of the Fermi energy level for quantum wire lasers. A comparison of this figure to Fig. 5 reveals two important results. One is that a higher differential gain can be obtained with the use of quantum wire structures. The second one is that the dependence of the differential gain on the Fermi energy level is enhanced for quantum wire lasers compared to quantum well lasers. A higher differential gain, therefore, is obtained in a quantum wire laser with a large number of quantum wires, and the sensitivity of the differential gain to the number is more enhanced for quantum wire lasers compared to the quantum well lasers.

One curve in Fig. 13 shows the f_r as a function of the dimension of the quantum wires. In this calculation, it is assumed that the two quantum dimensions are equal and that the number of quantum wires is optimized for each quantum dimension. This result indicates that f_r is enhanced by a factor of 3 with the use of thin quantum wires compared to the conventional DH. The spectral properties of the quantum wire laser are also improved. The second curve in Fig. 12 shows the dependence of α on the Fermi energy level. As shown in this figure, the dependence of α in a quantum wire laser is not as enhanced and is almost constant in the whole range. The second curve in Fig. 13 shows $\Delta\nu$ as a function of the thickness of the quantum wells. This indicates that α is reduced with the decrease of the thickness.

The α parameter of quantum box lasers should be noted. If we can ignore higher subbands' effect, the density of states is a δ function-like. Therefore, the photon energy with the maximum gain coincides with the energy levels, which leads to the disappearance of the detuning and the real part of the complex susceptibility becomes zero. Consequently, α is expected to be extremely small in a quantum box laser with a simultaneous improvement of f_r.

B. Magnetic Field Experiment

A quasi-quantum wire effect in a semiconductor laser can be realized through the use of high magnetic fields [8], [9], in which case electrons can move freely only in the direction of the magnetic field. The motion of such electrons is quantized in the two transverse directions (x, y), forming a series of Landau energy subbands. The density of states for the system $\rho_c(\epsilon)$ can be expressed as

$$\rho_c(\epsilon) = (\hbar\omega_c)\left(\frac{2m_c}{\hbar^2}\right)^{3/2} \sum_{j=0}^{\infty} \frac{1}{\sqrt{\epsilon - (j + \frac{1}{2})\hbar\omega_c}} \quad (26)$$

where ω_c and m_c are the cyclotron corner frequency and the effective mass of electrons. When $\hbar\omega_c$ is large enough (i.e., the B field is large enough), only the first Landau subband is occupied, resulting in a true one-dimensional electronic system. In the actual system, the carrier relaxation effect should also be considered.

Fig. 14 shows the measured spectral linewidth at 190 K for various magnetic fields (B = 0, 11, 16, 19 tesla) as a function of the reciprocal mode power $1/P$ [94]. A GaAlAs buried heterostructure laser grown by liquid phase epitaxy was operated in a stationary magnetic field of up to 19 tesla at 190 K. The test laser (an ORTEL Corporation experimental model) has a 0.15 μm active region thickness, 3 μm stripe width, and was 300 μm long. As

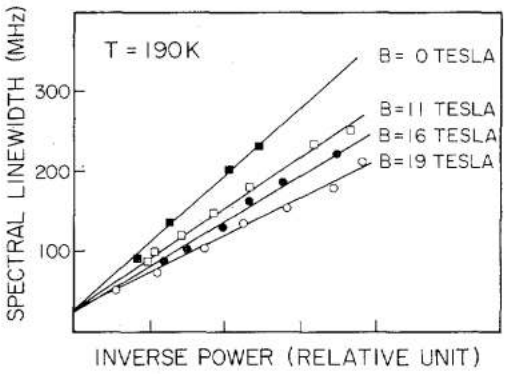

Fig. 14. The measured spectral linewidth as a function of the reciprocal of output power (in relative units) for magnetic fields of $B = 0$, 11, 16, and 19 tesla at 190 K.

shown in the figure, the measured linewidth for each magnetic field varies linearly with the reciprocal mode power. Such a variation indicates that the linewidth results from quantum broadening (spontaneous emission). The experimental results indicate that this power-dependent linewidth is substantially reduced with the increase of the magnetic field. At 19 tesla, the linewidth decreases by a factor of 0.6 compared to the linewidth without a magnetic field. This improvement of the power-dependent linewidth is believed to be due mainly to quantum wire effects through the formation of a quasi-one-dimensional electronic system as discussed above.

One important difference between "true" quantum wire structures and the quasi-quantum wires due to magnetic fields is that the optical confinement factor for true quantum wire structures can be controlled by varying the number of quantum wires. Theoretical predictions indicate that a higher Fermi energy level for laser oscillation leads to lower α and n_{sp} [7]. Therefore, in the true quantum wire case, it should be possible to decrease n_{sp} and α by reducing the number of quantum wires while maintaining the one-dimensional electronic properties. This would allow one to reap the benefits of quantum wires in terms of smaller α's without paying a penalty in n_{sp}. The overall reduction of linewidth $\Delta\nu$ would then be much larger than demonstrated here.

f_r was also measured at room temperature [93]. Fig. 15 shows the measured f_r with and without a magnetic field of 20 tesla as a function of the square root of the output power P_0. Open circles ($B = 0$) and closed circle ($B =$ 20 tesla) indicate the measured f_r. The straight lines in the figure are drawn by the least square error method. Since, as shown in (16), f_r is proportional to $\sqrt{P_0}$, f_r should lie on a straight line. The variation of the slope of this line will mainly reflect the change in differential gain g' which has resulted from the applications of the magnetic field. We notice that f_r with $B = 20$ tesla is enhanced 1.4 times compared to f_r with $B = 0$. From this change, we can estimate that g' ($B = 20$ tesla) is 1.9 times larger than g' ($B = 0$).

Quantum box effects (i.e., full quantization) were also investigated by Arakawa *et al.* [95] by placing a GaAs/

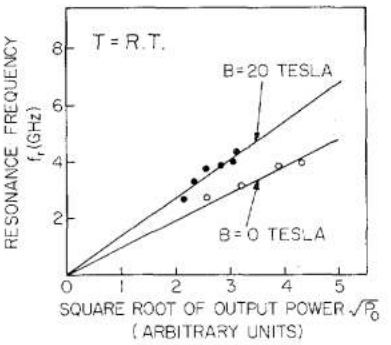

Fig. 15. The measured relaxation resonance frequency as a function of the square root of output power (in relative units) for magnetic fields of $B = 0$, 20 tesla at room temperature.

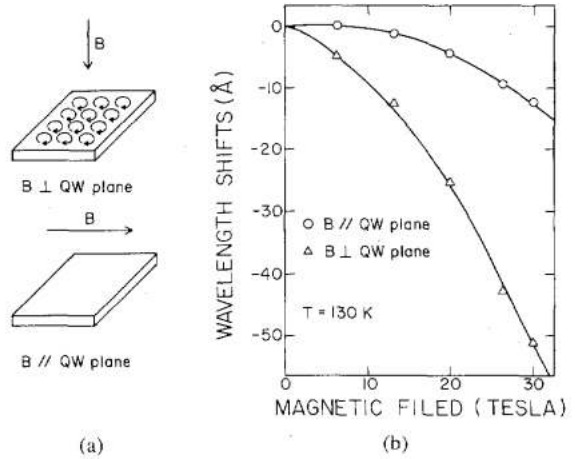

Fig. 16. (a) Electron motions confined by the quantum well potential as well as Lorentzian force, being in zero-dimensional electronic states. (b) Experimental results of the wavelength shift of the spontaneous emission spectrum as a function of the pulsed magnetic field up to 30 tesla.

GaAlAs quantum well laser in a high magnetic field. If a magnetic field is applied perpendicular to the quantum well plane as shown in Fig. 16(a), electrons are confined by the quantum well potential as well as the Lorentzian force, being in zero-dimensional electronic states. In this case, the density of states is described by the following formula:

$$\rho_c(\epsilon) = (\hbar\omega_c)\left(\frac{2m_c}{\hbar^2}\right)\sum_{k=0}^{\infty}\sum_{j=l,h}\sum_{n=1}^{\infty} \cdot \delta\left(\epsilon - \epsilon_{c_n}^{j} - \left(k + \frac{1}{2}\right)\hbar\omega_c\right). \quad (27)$$

The evidence of the formation of the full quantized effects was obtained by measuring anistropic properties of the spectral shift with the increase of the magnetic field. If a magnetic field is applied parallel to the QW plane, the cyclotron motion is interrupted by the QW potentials. Therefore, as long as the magnetic field is not extremely strong, the spectral peak shift is suppressed. On the other hand, with the perpendicular magnetic field, the spectral peak shift occurs towards a shorter wavelength through the increase of the Landau energy level. Fig. 16(b) is the experimental results of the wavelength shift of the spon-

taneous emission spectrum as a function of the pulsed magnetic field up to 30 tesla. The results clearly indicate the anisotropic properties, which is the evidence of the formation of the zero-dimensional electron states.

VII. Conclusions

We have discussed a number of interesting theoretical and experimental results of quantum well lasers with emphasis on the basic physical phenomena involved in the gain, the spectral fields, and the modulation response. The results reveal that an optimized use of the quantum well structure can lead to substantial improvement in most of the important properties of these devices.

References

[1] L. Esaki and R. Tsu, "Superlattice and negative differential conductivity in semiconductor lasers," *IBM. J. Res. Develop.*, vol. 14, pp. 61–68, 1970.

[2] R. Dingle, A. C. Gossard, and W. Wiegmann, "Direct observation of super lattice formation in a semiconductor heterostructure," *Phys. Rev. Lett.*, vol. 34, pp. 1327–1330, 1975.

[3] J. P. van der Ziel, R. Dingle, R. C. Miller, W. Wiegmann, and W. A. Nordland Jr., "Laser oscillation from quantum well states in very thin GaAl-$Al_{0.2}Ga_{0.8}As$ multilayer structures," *Appl. Phys. Lett.*, vol. 26, pp. 463–465, 1975.

[4] N. Holonyak, Jr., R. M. Kolbas, R. D. Dupuis, and P. D. Dapkus, "Quantum-well heterostructure lasers," *IEEE J. Quantum Electron.*, pp. 170–181, 1980.

[5] W. T. Tsang, "Extremely low threshold (AlGa)As modified multiquantum well heterostructure lasers grown by molecular beam epitaxy," *Appl. Phys. Lett.*, vol. 39, pp. 786–788, 1981.

[6] T. Fujji, S. Yamakoshi, K. Nanbu, O. Wada, and S. Hiyamizu, "MBE growth of extremely high-quality GaAs-AlGaAs GRIN-SCH lasers with a superlattice buffer layer," *J. Vac. Sci. Technol.*, vol. 2, pp. 259–261, 1984.

[7] R. Chin, N. Holonyak, Jr., B. A. Bojak, K. Hess, R. D. Dupuis, , and P. D. Dapkus, "Temperature dependence of threshold current for quantum well $Al_xGa_{1-x}As$-GaAs heterostructure laser diodes," *Appl. Phys. Lett.*, vol. 36, pp. 19–21, 1979.

[8] K. Hess, B. A. Bojak, N. Holonyak, Jr., R. Chin, and P. D. Dapkus, "Temperature dependence of threshold current for a quantum-well heterostructure laser," *Solid-State Electron.*, vol. 23, pp. 585–589, 1980.

[9] Y. Arakawa and H. Sakaki, "Multiquantum well laser and its temperature dependence of the threshold current," *Appl. Phys. Lett.*, vol. 40, pp. 939–941, 1982.

[10] Y. Arakawa, K. Vahala, and A. Yariv, "Quantum noise and dynamics in quantum well and quantum wire lasers," *Appl. Phys. Lett.*, vol. 45, pp. 950–952, 1984.

[11] Y. Arakawa, and A. Yariv, "Theory of gain, modulation response, and spectral linewidth in AlGaAs quantum well lasers," *IEEE J. Quantum Electron.*, vol. QE-21, pp. 1666–1674, 1985.

[12] Y. Arakawa, K. Vahala, and A. Yariv, "Dynamic and spectral properties in semiconductor lasers with quantum well and wire effects," presented at the 2nd Int. Conf. Modulated Semiconductor Structures, Kyoto, Japan, 1985.

[13] Y. Arakawa, A. Larsson, J. Paslaski, and A. Yariv, "Active *Q*-switching in a multiquantum well laser with an internal loss modulation," submitted to *Appl. Phys. Lett.*

[14] H. Kromer and H. Okamoto, "Some design consideration for multiquantum-well lasers," *Japan. J. Appl. Phys.*, vol. 23, pp. 970–972, 1984.

[15] A. Yariv, C. Lindsey, and U. Sivan, "Approximate analytic solution for electronic wave function and energies in coupled quantum wells," *J. Appl. Phys.*, vol. 58, pp. 3669–3671, 1985.

[16] R. Lang and K. Nishi, "Electronic localization in a semiconductor superlattice,," *Appl. Phys. Lett.*, vol. 45, pp. 98–100, 1984.

[17] D. Kasemset, C. S. Hong, N. B. Patel, and D. Dapkus, "Graded barrier single quantum well lasers—Theory and experiment," *IEEE J. Quantum Electron.*, vol. QE-19, pp. 1025–1030, 1983.

[18] A. Sugimura, "Threshold current for AlGaAs quantum well lasers," *IEEE J. Quantum Electron.*, vol. QE-20, pp. 336–343, 1984.

[19] P. T. Landsberg. M. S. Abrahams, and M. Olsinski, "Evidence of no *k*-selection in gain spectra of quantum well AlGaAs laser diodes," *IEEE J. Quantum Electron.*, vol. QE-21, pp. 24–28, 1985.

[20] N. K. Dutta, "Calculated threshold current of GaAs quantum well lasers," *J. Appl. Phys.*, vol. 53, pp. 7211–7214, 1982.

[21] ——, "Current injection in multiquantum well lasers," *IEEE J. Quantum Electron.*, vol. QE-19, pp. 794–797, 1983.

[22] M. Yamada, S. Ogita, M. Yamagishi, and K. Tabata, "Anisotropy and broadening of optical gain in a GaAs/AlGaAs multiquantum-well laser," *IEEE J. Quantum Electron.*, vol. QE-21, pp. 640–645, 1985.

[23] M. Yamada, K. Tabata, S. Ogita, and M. Yamagishi, "Calculation of lasing gain and threshold current in GaAsAlGaAs mutiquantum well lasers," *Trans. IECE Japan*, vol. E68, pp. 102–108, 1984.

[24] Y. Arakawa, H. Sakaki, M. Nishioka, J. Yoshino, and T. Kamiya," Recombination lifetime of carriers in GaAs-GaAlAs quantum wells near room temperature," *Appl. Phys. Lett.*, vol. 46k, pp. 519–521, 1985.

[25] N. K. Dutta, R. L. Hartman, and W. T. Tsang, "Gain and carrier lifetime measurement in AlGaAs single quantum well lasers," *IEEE J. Quantum Electron.*, vol. QE-19, pp. 1243–1246, 1983.

[26] Casey and Panish, *Heterostructure Lasers, Part A*. New York: Academic, 1978.

[27] H. Kobayaski, H. Iwamura, T. Saku, and K. Otsuka, "Polarization dependent gain-current relationship in GaAs-AlGaAs MQW laser diodes," *Electron. Lett.*, vol. 19, pp. 166–168, 1983.

[28] M. Asada, A. Kameyama, and Y. Suematsu, "Gain and intervalenceband absorption in quantum-well lasers," *IEEE J. Quantum Electron.*, vol. QE-20, pp. 745–753, 1984.

[29] M. Yamanishi and I. Suemune, "Comments on polarization dependent momentum matrix elements in quantum well lasers," *Japan. J. Appl. Phys.*, vol. 23, pp. L35–L36, 1984.

[30] E. O. Kane, "Band structure of indium antimonide," *J. Phys. Chem. Solids*, pp. 249–269, 1957.

[31] A. Sugimura, "Auger recombination effect on threshold current of InGaAsP quantum well lasers," *IEEE J. Quantum Electron.*, vol. QE-19, pp. 932–941, 1983.

[32] N. K. Dutta, "Calculation of Auger rates in a quantum well structure and its application to InGaAsP quantum well lasers," *J. Appl. Phys.*, vol. 54, pp. 1236–1245, 1983.

[33] L. C. Chiu and A. Yariv, "Auger recombination in quantum-well InGaAsP heterostructure lasers," *IEEE J. Quantum Electron.*, vol. QE-18, pp. 1406–1409, 1982.

[34] C. Smith, R. A. Abram, and M. G. Burt, "Auger recombination in long wavelength quantum-well lasers," *Electron. Lett.*, 1984.

[35] Y. Arakawa, A. Larsson, M. Mittelstein, and A. Yariv," Observation of gain flattening and second subband laser oscillation in a single quantum well laser," unpublished.

[36] R. D. Dupis, P. D. Dapkus, N. Holonyak, Jr., E. A. Rezek, and R. Chin, "Room-temperature laser operation of quantum well $Ga_{1-x}Al_xAs$-GaAs laser diodes by metal organic chemical vapor deposition," *Appl. Phys. Lett.*, vol. 32, pp. 292–297, 1978.

[37] W. T. Tsang, C. Weisbuch, R. C. Miller, and R. Dingle, "Curent injection GaAS-$Al_xGa_{1-x}As$ multiquantum well heterostructure lasers prepared by molecular beam epitaxy," *Appl. Phys. Lett.*, vol. 35, pp. 673–675, 1979.

[38] W. T. Tsang, "A graded-index waveguide separate-confinement laser with very low threshold and a narrow Gaussian beam," *Appl. Phys. Lett.*, vol. 39, pp. 134–136, 1981.

[39] P. Blood, E. D. Fletcher, and K. Woodbridge, "Dependence of threshold current on the number of wells in AlGaAs-GaAs quantum well lasers," *Appl. Phys. Lett.*, vol. 47, pp. 193–195, 1985.

[40] S. D. Harsee, M. Baldy, P. Assenat, B. de Cremoux, and J. P. Duchemin," Very low threshold GRIN-SCH GaAs/AlGaAs laser structure grown by OM-VPE," *Electron. Lett.*, vol. 18, pp. 1095–1097, 1982.

[41] D. R. Scifres, R. D. Burham, and W. Streifer, "High power coupled multiple strip quantum well injection lasers," *Appl. Phys. Lett.*, pp. 118–120, 1982.

[42] J. P. van der Ziel, H. Temkin, and R. D. Dupis, "High-power picosecond pulse generation in GaAs multiquantum well phase-locked laser arrays using pulsed current injection," *IEEE J. Quantum Electron.*, vol. QE-20, pp. 1236–1242, 1984.

[43] O. Wada, T. Sanada, M. Kuno, and T. Fujii, "Very low threshold current ridge-waveguide AlGaAs/GaAs single-quantum-well lasers," *Electron. Lett.*, 1985.

[44] E. A. Rezek, N. Holonyak, Jr., and B. K. Fuller, "Temperature dependence of threshold current for coupled multiple quantum well $In_{1-x}Ga_xP_{1-z}As_z$-InP heterostructure laser diodes," *J. Appl. Phys.*,

vol. 51, pp. 2402–2405, 1980.
[45] H. Temkin, K. Alavi, W. R. Wagner, T. P. Pearsall, and A. Y. Cho," 1.5-16 μm $Ga_{0.47}In_{0.53}As/Al_{0.48}$ multiquantum well laser grown by molecular beam epitaxy," *Appl. Phys. Lett.*, vol. 42, pp. 845–847, 1983.
[46] T. Yanase, Y. Kato, I. Mito, M. Yamaguchi, K. Nishi, K. Kobayashi, and R. Lang, "1.3 μm InGaAsP/InP multiquantum-well laser grown by vapour-phase epitaxy," *Electron. Lett.*, vol. 19, pp. 700–701, 1983.
[47] N. K. Dutta, T. Wessel, N. A. Olsson, R. A. Logan, R. Yen, and P. J. Anthony," Fabrication and performance characteristics of InGaAsP ridge-guide distributed-feedback multiquantum-well lasers," *Electron Lett.*, vol. 21, pp. 571–573, 1985.
[48] Y. Kawamura, H. Asahi, and K. Wakita, "InGaAs/InGaAlAs/InAlAs/InP SCH-MQW laser diodes grown by molecular beam epitaxy," *Electron Lett.*, vol. 20, pp. 459–460, 1984.
[49] Y. Ohmori, Y. Suzuki, and H. Okamoto, "Room temperature CW operation of GaSb/AlGaSb MQW laser diodes grown by MBE," *Japan. J. Appl. Phys.*, vol. 24, pp. L657–659, 1985.
[50] A. Larsson, M. Mittelstein, Y. Arakawa, and A. Yariv," High efficiency broad area single quantum well laser with narrow single-lobed far-field patterns prepared by molecular beam epitaxy," *Electron. Lett.*, vol. 22, pp. 79–81, 1986.
[51] T. Ikegami and Y. Suematsu, "Direct modulation semiconductor junction lasers," *Electron. Commun. Japan*, vol. B51, pp. 51–58, 1968.
[52] T. P. Paoli and J. E. Ripper, "Direct modulation of semiconductor lasers," *Proc. IEEE*, vol. 58, p. 1457, 1970.
[53] K. Y. Lau, N. Bar-Chaim, I. Ury, C. Harder, and A. Yariv, "Direct amplitude modulation of short cavity lasers up to *X*-band frequency," *Appl. Phys. Lett.*, vol. 43, pp. 1–3, 1983.
[54] K.Y. Lau, N. Bar-Chaim, I. Ury, and A. Yariv, "An 11 GHz direct modulation bandwidth GaAlAs window laser on semi-insulating substrate operating at room temperature," *Appl. Phys. Lett.*, vol. 45, pp. 345–347, 1984.
[55] K. Y. Lau and A. Yariv, "Ultra-high speed semiconductor lasers," *IEEE J. Quantum Electron.*, vol. QE-21, p. 121, 1985.
[56] K. Vahala and A. Yariv, "Detuned loading in couple cavity semiconductor lasers—Effects on quantum noise and dynamics," *Appl. Phys. Lett.*, vol. 45, pp. 501–503, 1984.
[57] K. Uomi, N. Chinone, T. Ohyoshi, and T. Kajimura, "High relaxation oscillation freqeuncy (beyond 10 GHz) of GaAlAs multiquantum well lasers," *Japan. J. Appl. Phys.*, vol. 24, pp. L539–L541, 1985.
[58] K. Kobayashi, H. Iwamura, T. Saku, K. Otsuka, and H. Okamoto," Dynamic behavior of a GaAs-AlGaAs MQW laser diode," *Electron. Lett.*, vol. 19, pp. 166–167, 1983.
[59] M. W. Fleming and A. Mooradian, "Fundamental line broadening of single mode (GaAl)As diode lasers," *Appl. Phys. Lett.*, vol. 38, pp. 511–513, 1981.
[60] C. Henry, "Theory of the linewidth of semiconductor," *IEEE J. Quantum Electron.*, vol. QE-18, pp. 259–264, 1982.
[61] K. Vahala and A. Yariv, "Semiclassical theory of noise in semiconductor lasers—Part I," *IEEE J. Quantum Electron.*, vol. QE-18, pp. 1096, 1101, 1982.
[62] ——, "Semiclassical theory of noise in semiconductor lasers—Part II, "*IEEE J. Quantum Electron.*, vol. QE-18, pp. 1102–1109, 1982.
[63] M. G. Burt, "Linewidth enhancement factor for quantum well laser," *Electron. Lett.*, vol. 20 pp. 27–28, 1984.
[64] K. Vahala, L. C. Chiu, S. Margalit, and A. Yariv," On the linewidth enchancement factor α in semiconductor injection lasers," *Appl Phys. Lett.*, vol. 42, pp. 531–633, 1983.
[65] Y. Arakawa and A. Yariv, "Fermi energy dependence of linewidth enhancement factor," *Appl. Phys. Lett.*, vol. 47, pp. 905–907, 1985.
[66] N. Ogasawara, R. Itoh, and R. Morita, "Linewidth enhancement factor in GaAs/AlGaAs multiquantum well lasers," *Japan. J. Appl. Phys.*, vol. 24, pp. L519–L521, 1985.
[67] T. H. Wood, C. A. Burrus, D. A. B. Miller, D. S. Chemla, T. C. Damen, A. C. Gossard, and W. Wiegmann," High-speed optical modulation with GaAs/GaAlAs quantum wells in a p-i-n diode structure," *Appl Phys. Lett.*, vol. 44, pp. 16–18, 1984.
[68] T. H. Wood, C. A. Burrus, R. S. Tucker, J. S. Weiner, D. A. B. Miller, D. S. Chemla, T. C. Damen. A. C. Gossard, and W. Wiegmann, *Electron. Lett.*, vol. 21, pp. 693–695, 1985.
[69] D. A. B. Miller, D. S. Chemla, T. C. Damen, A. C. Gossard, W. Wiegmann, T. H. Wood, and C. A. Burrus," Novel hybrid optically bistable switch: The quantum well self-optic effect device," *Appl. Phys. Lett.*, vol. 45, pp. 13–15, 1984.
[70] T. H. Wood, C. A. Burrus, A. H. Gnauck, J. M. Wiesenfeld, D. A. B. Miller, D. S. Chemla, and T. C. Damen," *Appl. Phys. Lett.*, vol. 47, pp. 190–192, 1985.
[71] A. Larsson, A. Yariv, R. Tell, J. Maserjian, and S. T. Eng, "Spectral and temporal characterisitcs of AlGaAs/GaAs superlattice p-i-n photodetectors," *Appl. Phys. Lett.*, vol. 47, pp. 866–868, 1985.
[72] C. Y. Chen, "New minority hole sinked photoconductive detector," *Appl. Phys. Lett.*, vol. 43, pp. 1115–1117, 1983.
[73] K. Kaede, Y. Arakawa, P. Derry, J. Papaslaski, and A. Yariv," High speed GaAs/AlGaAs photoconductive detector using a p-modulation doped superlattice," *Appl. Phys. Lett.*, vol. 48, pp. 1096–1097, 1986.
[74] M. Yamanishi and M. Suemune, "Quantum mechanical size effect modulation light source—A new field effect semiconductor laseror light emitting diode," *Japan. J. Appl. Phys.*, vol. 22, p. L22, 1983.
[75] K. Tsukada and C. L. Tang, "*Q*-switching of semiconductor lasers," *IEEE J. Quantum Electron.*, vol. QE-13, pp. 37–43, 1977.
[76] M. Yamanishi, K. Ishii, M. Ameda, and T. Kawamura, "High speed repetitive *Q*-switching in acoustic distributed feedback lasers," *Japan. J. Appl. Phys.*, suppl. 17, pp. 359–363, 1978.
[77] D. Z. Tsang, J. N. Walpole, S. H. Groves, J. J. Hsieh, and J. P. Donnelly, "Intracavity loss modulation of GaInAsP diode lasers," *Appl. Phys. Lett.*, vol. 38, p. 120, 1981.
[78] D. Z. Tsang and J. N. Walpole, "*Q*-switched semiconductor diode lasers," *IEEE J. Quantum Electron.*, vol. QE-19, p. 145, 1983.
[79] D. Z. Tsang, J. N. Walpole, Z. L. Liau, S. H. Groves, and V. Diadiuk, "*Q* switching of low threshold buried heterostructure diode laser at 10 GHz," *Appl. Phys. Lett.*, vol. 45, p. 204, 1984.
[80] P. T. Ho. L. A. Glasser, E. P. Ippen, and H. A. Haus, "Picosecond pulse generation with a CW GaAlAs laser diodes," *Appl. Phys. Lett.*, vol. 33, pp. 241–242, 1978.
[81] J. P. van der Ziel, R. A. Logan, and R. M. Mikulyak, "Generation of subpicosecond pulse from an actively mode locked GaAs laser in an external ring cavity," *Appl. Phys. Lett.*, vol. 39, pp. 867–869, 1981.
[82] H. Ito, H. Yokoyama, S. Murata, and H. Inaba, "Picosecond optical pulse generation from r.f. modulated AlGaAs DH diode laser," *Electron. Lett.*, vol. 15, p. 738, 1979.
[83] G. J. Aspin, J. E. Carrol, and R. G. Plumb," The effect of cavity length on picosecond pulse generation with high rf modulated AlGaAs double heterostructure lasers," *Appl. Phys. Lett.*, vol. 39, p. 860, 1981.
[84] D. A. B. Miller, D. S. Chemla, T. C. Damen, A. C. Gossard, W. Wiegmann, T. H. Wood, and C. A. Burrus," Bandedge electroabsorption in quantum well structure: The quantum confined Stark effect," *Phys. Rev. Lett.*, vol. 53, pp. 2173–2177, 1984.
[85] J. S. Weiner, D. A. B. Miller, D. S. Chemla, T. C. Damen, C. A. Burrus, T. H. Wood, A. C. Gossard, and W. Wiegman, *Appl. Phys. Lett.*, vol. 47, p. 1148, 1985.
[86] S. Tarucha, H. Kobayashi, Y. Horikoshi, and X. Okamoto, "Carrier induced energy-gap shrinkage in current injection GaAs/AlGaAs MQW heterostructures," *Japan. J. Appl. Phys.*, vol. 23, pp. 874–881, 1984.
[87] Asada and Suematsu, *Japan. J. Appl. Phys.*, vol. 24, pp. L93–L95, 1985.
[88] Petroff, "Toward quantum well wires: Fabrication and optical properties," vol. 41, pp. 635–637, 1982.
[89] H. Sakaki, "Scattering suppression and high mobility effect of single quantum electrons in ultrafine semiconductor wire structure," *Japan. J. Appl. Phys.*, vol. 20, pp. L91–L93, 1981.
[90] Y. Arakawa, H. Sakaki, M. Nishioka, and N. Miura, "Two dimensional quantum-mechanical confinement of electrons in semiconductor lasers by strong magnetic fields," *IEEE J. Quantum Electron.*, vol. QE-18, pp. 10–17, 1983.
[91] ——, "Two-dimensional quantum-mechanical confinement of electrons in light emitting diodes by strong magnetic fields," *IEEE Trans. Electron Devices*, vol. ED-30, pp. 330–338, Apr. 1983.
[92] H. J. A. Bluyssen and L. J. van Ruyven, "Operation of a double heterojunction GaAs/AlGaAs injection laser with a p-type active layer in a strong magnetic field," *IEEE J. Quantum Electron.*, vol. QE-16, pp. 29–33, 1983.
[93] Y. Arakawa, K. Vahala, A. Yariv, and K. Lau, "Enhanced modulation bandwidth of GaAlAs double heterostructure lasers in high magnetic fields: Dynamic response with quantum wire effects," *Appl. Phys. Lett.*, vol. 47, pp. 1142–1144, 1985.
[94] ——, "Reduction of the spectral linewidth of semiconductor lasers

with quantum wire effects—Spectral properties of GaAlAs double heterostructure lasers," *Appl. Phys. Lett.*, vol. 48, pp. 384–386, 1986.
[95] Y. Arakawa, H. Sakaki, M. N. Nishioka, H. Okamoto, and N. Miura, "Spontaneous emission characteristics of quantum well lasers in strong magnetic fields—An approach to quantum box light source," *Japan. J. Appl. Phys.*, vol. 22, pp. L804–L806, 1985.

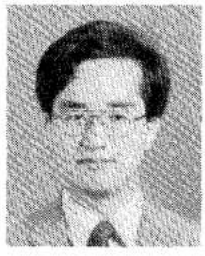

Yasuhiko Arakawa (S'77–M'80) was born in Aichi Prefecture, Japan, on November 26, 1952. He received the B.S., M.S., and Ph.D. degrees in electrical engineering from the University of Tokyo, Tokyo, Japan, in 1975, 1977, and 1980, respectively.

In the graduate school, he conducted research on optical communication theory. In 1980, he joined the Institute of Industrial Science, University of Tokyo, as an Assistant Professor and is currently an Associate Professor. After 1980, he extended his speciality to optical device research. His current research includes dynamic and noise properties of quantum well lasers, basic investigation of quantum wire and quantum box lasers using high magnetic fields, and fabrication of new optical devices using quantum well structures. From 1984 to 1986, he was Visiting Scientist at the California Institute of Technology, Pasadena, doing research in collaboration with Professor A. Yariv.

In 1980 Dr. Arakawa was awarded the Niwa Memorial Prize. In 1981 and 1983, he was also awarded the Excellent Paper Award and the Young Scientist Award, respectively, from Institute of Electronics and Communication Engineers of Japan. He is a member of the Institute of Electronics and Communication Engineers of Japan and the Japan Society of Applied Physics.

Amnon Yariv (S'56–M'59–F'70), for a photograph and biography, see p. 448 of the March 1986 issue of this JOURNAL.